AD NUMBER

AD808780

NEW LIMITATION CHANGE

TO

Approved for public release, distribution unlimited

FROM

Distribution authorized to DoD only; Administrative/Operational Use; FEB 1967. Other requests shall be referred to U.S. Army Electronics Command, Attn: AMSEL-KL-PC, Fort Monmouth, NJ 07703-5601.

AUTHORITY

Army Electronics Command ltr dtd 1 May 1968

TECHNICAL REPORT ECOM-01996-2

INVESTIGATION OF HYDRAZINE-AIR FUEL CELL SYSTEMS

Progress Report No. 2

by

Seigo Matsuda, Sarah P. Brown,
John O. Smith, and Bernard P. Sullivan

February 1967

ECOM

UNITED STATES ARMY ELECTRONICS COMMAND · FORT MONMOUTH, N.J.
Contract DA 28-043-AMC-01996 (E)
MONSANTO RESEARCH CORPORATION
BOSTON LABORATORY
EVERETT, MASSACHUSETTS 02149

NOTICES

Disclaimers

The findings in this report are not to be construed as an official Department of the Army position, unless so designated by other authorized documents.

The citation of trade names and names of manufacturers in this report is not to be construed as official Government indorsement or approval of commercial products or services referenced herein.

Disposition

Destroy this report when it is no longer needed. Do not return it to the originator.

Technical Report ECOM-01996-2 February 1967

INVESTIGATION OF HYDRAZINE-AIR FUEL CELL SYSTEMS

Progress Report No. 2
15 May 1966 to 12 August 1966

Contract No. DA28-043-AMC-01996(E)
Task No. 1C6-22001-A-053-04-12

Prepared By

S. Matsuda, S. P. Brown,
J. O. Smith and B. P. Sullivan

Monsanto Research Corporation
Boston Laboratory
Everett, Massachusetts 02149

for

U. S. Army Electronics Command
Fort Monmouth, New Jersey

MRB403502

SUMMARY

Fuel efficiency of the hydrazine-air fuel cell system can be significantly increased by selecting a proper electrode substrate. It must be a poor hydrogen electrode material, according to the mixed potential concept. Both the anode potential and the fuel efficiency were improved by applying a minute amount of catalyst poisons such as $S^=$ and $Se^=$. The anode potential was increased by increasing the concentration of KOH and N_2H_4 in the electrolyte. The anode potential was not affected by Cl^- up to 200 mg/l, but it was lowered by $CO_3^=$ and Fe^{++} in the electrolyte.

NH_3 in the exhaust gas from the anode was satisfactorily decomposed by Pt catalyst. In addition to fuel cell grade asbestos separator, which has given the best results, some non-asbestos separators such as ThO_2 membrane and alkaline battery separator also showed the promising results for the N_2H_4 - air system.

Publications, Lectures, Reports and Conferences

Conferences:

Date: 16 May 1966
Place: Monsanto Research Corporation, Boston Laboratory, Everett, Massachusetts

Present at this conference were Mr. J. Perry of the U. S. Army Electronics Command and Dr. S. Matsuda of Monsanto Research Corporation.

The results obtained during the first quarter and the plans for the second quarter were reviewed and discussed in detail.

TABLE OF CONTENTS

		Page
I.	INTRODUCTION	1
II.	PHASE I - INVESTIGATION OF HYDRAZINE ANODE	2
	A. BACKGROUND	2
	B. TASK I. STUDY OF ELECTRODE SUBSTRATE	5
	1. Experimental Results	5
	2. Discussion	6
	C. TASK II. STUDY OF ELECTROLYTE	7
	1. Background	7
	2. Experimental Method	7
	3. Effect of Concentration of KOH and N_2H_4	9
	4. Effect of Impurity Ions in the Electrolyte	9
	a. Effect of $CO_3^=$	9
	b. Effect of Cl^-	9
	e. Effect of Fe^{++}	9
	5. Conclusions	15
	D. TASK III. STUDY OF CATALYST POISONS	15
	1. Experimental Method	15
	2. Results on Solid Nickel Electrode	17
	3. Results on Porous Nickel Electrode	17
	4. Discussion	17
	E. TASK IV. STUDY OF INEXPENSIVE CATALYST	23
	F. TASK V. STUDY OF DECOMPOSITION OF NH_3	23
	1. Background	23
	2. Experimental Method	24
	3. Results	24
III.	PHASE II - INVESTIGATION OF SEPARATOR	30
	A. EXPERIMENTAL METHOD	30
	B. ASBESTOS SEPARATOR	30

TABLE OF CONTENTS (Cont.)

		Page
	C. NON-ASBESTOS SEPARATOR.	30
	D. DISCUSSION.	30
IV.	WORK PLANNED FOR THE THIRD QUARTER.	33
V.	REFERENCES.	34
VI.	IDENTIFICATION OF PERSONNEL	35

LIST OF ILLUSTRATIONS

Figure	Title	Page
1	Schematic Illustration on Hydrazine Electrode Reaction and Approaches for its Improvement, on the Basis of the Mixed Potential Concept	3
2	Half Cell for Polarization Study	8
3	Effect of KOH Concentration on Hydrazine Anode Potential (N_2H_4:2M)	10
4	Effect of Cl^- on the Hydrazine Electrode Potential (7M KOH + 2M N_2H_4)	13
5	Effect of Fe^{++} on the Hydrazine Electrode Potential (7M KOH + 2M N_2H_4)	14
6	Reaction Generator and Gas Collecting Train	16
7	Effect of $S^=$ in the Electrolyte on the Polarization Characteristics of Hydrazine Electrode (7M KOH + 2M N_2H_4)	18
8	Effect of $Se^=$ in the Electrolyte on the Polarization Characteristics of Hydrazine Electrode (7M KOH + 2M N_2H_4)	19
9	Effect of As^{5-} in the Electrolyte on the Polarization Characteristics of Hydrazine Electrode (7M KOH + 2M N_2H_4)	20
10	Effect of Catalyst Poisons on Gas Evolution Rate at Open Circuit Conditions	21
11	Schematic Diagram of an Apparatus for NH_3 Decomposition Test	25

LIST OF TABLES

Table	Title	Page
1	Analysis (%) of the Evolved Gas on Au-Pd Electrode in 5M KOH + 2M N_2H_4 at 70°C.	6
2	Effect of Concentration of KOH and N_2H_4 on the Hydrazine Anode Potential at 100 ma/cm2, volts vs SCE.	11
3	Effect of $CO_3^=$ in KOH Electrolyte	12
4	The Effect of the Catalyst Poisons on the Composition of the Evolved Gas at 100 ma/cm^2 Polarization. . . .	22
5	NH_3 Decomposition "1".	26
6	NH_3 Decomposition "2".	28
7	NH_3 Decomposition "3".	29
8	Summary of Separator Tests	31

I. INTRODUCTION

This is the second quarterly report on the investigation of hydrazine (N_2H_4) - air fuel cell systems under Contract DA-28-043-AMC-01996 (E) by U.S. Army Electronics Command, Power Sources Division, Electronic Components Laboratory.

The work is aimed at acquiring a basic understanding of the components of the cell, particularly of the anode. An additional objective is determination of ways to improve the presently operating systems by using the knowledge obtained during the contract.

It is then expected that these improvements will insure the power density, life time characteristics, and system design of hydrazine-air fuel cell systems for ground power applications, in the range of sixty watts to one kilowatt.

During the first quarter, some important determinations were made particularly concerning the mechanism of the hydrazine anode reaction. The mixed potential concept seemed to explain most properly the various characteristics observed on the hydrazine anode.

II. PHASE I-INVESTIGATION OF HYDRAZINE ANODE

A. BACKGROUND

In the first quarterly report, the mixed potential concept was suggested as the most probable mechanism for the hydrazine electrode reaction, which seemed to consist of multiple reduction-oxidation systems existing simultaneously on the electrode. On the basis of polarization data on the hydrazine electrodes under various conditions, the relation between two major red-ox systems, the hydrazine reaction (1) and the hydrogen reaction (2) were discussed in detail.

$$N_2H_4 + 4\ OH^- \rightleftarrows N_2 + 4\ H_2O + 4e \qquad (1)$$

$$4\ H_2O \rightleftarrows 4\ OH^- + 4\ H\ (ads)\ \text{or}\ 2\ H_2 - 4e \qquad (2)$$

Figure 1 (a) illustrates the most common relationship between two reactions such as that in 5M KOH + 2M N_2H_4 electrolyte at 50°C. The letters indicate the following:

N-Ox: Forward direction of reaction (1)

N-Red: Backward direction of reaction (1)

H-Ox: Backward direction of reaction (2)

H-Red: Forward direction of reaction (2)

$E_{o\text{-}N_2H_4}$: Equilibrium potential of the reaction (1) in the given system.

$E_{o\text{-}H_2}$: Equilibrium potential of reaction (2) in the given system.

E_o: The open circuit potential of the hydrazine electrode (mixed potential).

E: The potential of the hydrazine electrode at an apparent current density I in a cell with the air cathode.

$i_{o\text{-}N_2H_4}$: The exchange current for reaction (1).

$i_{o\text{-}H_2}$: The exchange current for reaction (2).

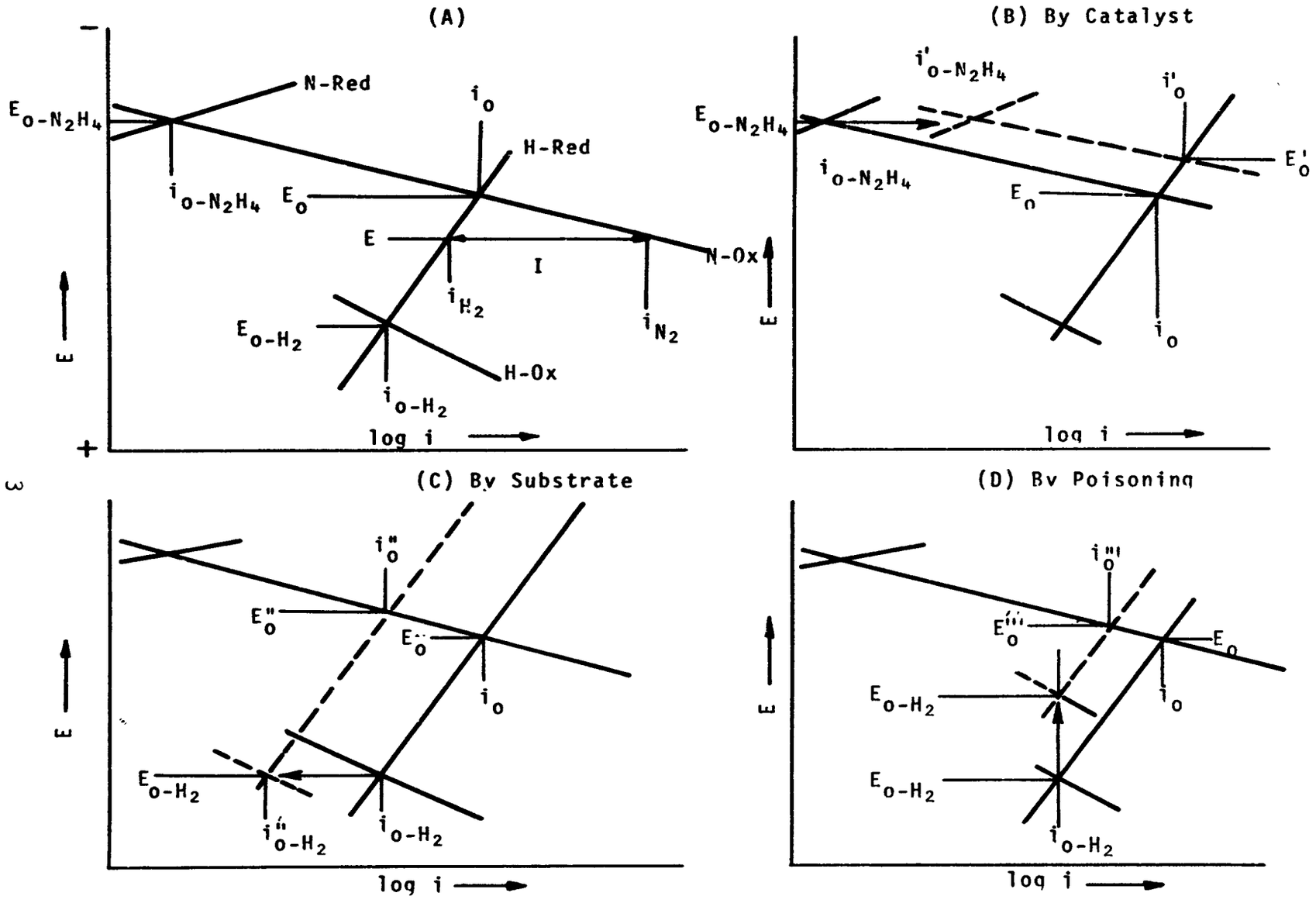

Figure 1. Schematic Illustration of Hydrazine Electrode Reaction and Approaches for its Improvement, on the Basis of the Mixed Potential Concept.

i_o: The local cell current between two electrodes (1) and (2) on the hydrazine anode at open circuit condition.

I: The apparent current in the hydrazine-air fuel cell which is utilized externally.

I practically equals $(i_{N_2} - i_{H_2})$ if the currents for N-Red and H-Ox are negligible. i_o corresponds to the rates of both N_2 and H_2 gas evolution at open circuit, and according to Faraday's law the rate of H_2 evolution should be twice that of N_2 evolution. i_{N_2} and i_{H_2} correspond, respectively, to the rates of N_2 evolution and of H_2 evolution at the potential E.

On the basis of this concept, three approaches can be taken to improvement of the performance of the hydrazine electrode. These approaches are illustrated in the other three figures in Figure 1.

The first approach is use of more active catalysts for N_2H_4 decomposition. The higher activity of catalysts contributes in general a higher $i_{o\text{-}N_2H_4}$ value and a lower polarization to the reaction (1), as shown in Figure 1 (b). These changes, however, result not only in a more active potential, E', but also in a higher i_o value, i_o'. In other words, the improvement of the potential will be obtained only with some loss of fuel efficiency. It should also be mentioned that the highly active catalysts for N_2H_4 decomposition are also very active catalysts for the hydrogen electrode reaction, so that the increase in i_o may become very detrimental while the improvement of E_o becomes much less.

The second approach is use of poor hydrogen electrode material as the electrode substrate. This approach can be clearly understood by discussing an analogous phenomenon known in metallic corrosion.

When the mixed potential concept is applied to explain the uniform corrosion of a piece of metal, such as the corrosion of iron in aerated water, the theory assumes that the area of the local anode equals the area of the local cathode. When a more noble metal such as copper is then attached to the iron, the local anode area becomes larger than the local cathode area on the iron

surface because the part of the local cathode area corresponding to the surface area of the copper piece is expected to become a more or less stationary anode. Since the corrosion rate of iron in aerated water is controlled by the diffusion of dissolved oxygen in the water and the difference in the kind of metal has relatively little influence on the rate of cathode reaction, the current density of the anode reaction remains practically unchanged, and the total rate of corrosion of iron increases with the increase of the local anode area. Consequently, when the surface area of the copper piece becomes equal to or larger than that of the iron piece, the corrosion rate reaches its maximum.

In the present case, analogous to the above, E_o and i_o in Figure 1 correspond to the corrosion potential and the corrosion rate of iron, and are controlled by the hydrogen electrode reaction (2) which has a higher slope on the polarization curve than reaction (1). But it is strongly affected by the kind and condition of the electrode material. Consequently, if we can assume the condition that the electrode substrate surface acts mainly as the hydrogen electrode (reaction (2)), the use of a proper electrode substrate having a poor hydrogen electrode activity and a sufficiently large surface area is expected to provide more desirable values of E_o and i_o. Figure 1 (c) illustrates an improvement in both values of E_o and i_o to E_o'' and i_o'' by lowering the exchange current of the hydrogen electrode from i_o to $i''_{o\text{-}H_2}$.

The third approach is to add a small amount of catalyst poison to the system. The amount of hydrogen cathodically charged into a metal is increased significantly by the presence of a small amount of a catalyst poison such as $S^=$, $Se^=$ and $P^=$ in the electrolyte. Iron cathodically charged with hydrogen in the presence of $S^=$ ion in the electrolyte showed a more active potential than that for one without the treatment in subsequent corrosion tests. (Ref. 1). It is believed that these catalyst poisons slow down the rate of recombination of hydrogen atoms to molecular hydrogen and cause the accumulation of hydrogen in metals. The higher concentration of the accumulated hydrogen on the electrode surface provides a more negative potential than the standard potential for reaction (2). Consequently, the presence of a small amount of catalyst poison in the electrolyte should result in a higher E_o value and a lower i_o, as illustrated in Figure 1 (d).

B. TASK I. STUDY OF ELECTRODE SUBSTRATE

1. Experimental Results

During the second quarter, pure gold was examined as an electrode substrate. Squares (2 x 2 in.) of 0.001 in. thick gold foil were first heat-treated for 10 minutes in air at 600°C and then were plated with 10 mg/in^2 of Pd black by electrolysis. Electrode potentials and results of analysis of the evolved gas at various current densities in 5M KOH + 2M N_2H_4 at 70°C are summarized in Table 1.

The potentiostatic sweep curve on this electrode at the rate of 2000 mV/hr indicated a hydrogen absorption peak both in 5M KOH + 2M N_2H_4 and in 5M KOH with bubbling hydrogen over the electrode.

Table 1

ANALYSIS (%) OF THE EVOLVED GAS ON AU-PD ELECTRODE IN 5M KOH + 2M N_2H_4 AT 70°C.

	Current Density, ma/cm^2			
	12.5	25	50	100
H_2	0	0	0	0.7
N_2	>99.5	>99.5	>99.5	99.3
NH_3	0.06	0.05	0.05	0.05
Electrode Potential*	-0.93	-0.92	-0.91	-0.91

*Volts vs. SCE

In order to determine more clearly the effect of galvanic coupling, 2 x 2 in. gold foil without Pd black was connected through a palladium wire to 2 x 2 in. palladium foil plated with 10 mg/in^2 of Pd black and were polarized together against the Pt dummy electrodes in the electrolyte. The potentials of the gold foil and palladium foil were identical (-0.97 volt vs SCE) for all current densities tested up to 100 ma/cm^2.

The rate of gas evolution at open circuit condition was extremely low, and the rates at various current densities were close to the theoretical rate according to Faraday's law for the oxidation of N_2H_4 by equation (1). Analysis of the evolved gas also showed none or very little hydrogen (average less than 2%) and a very low NH_3 content (average 0.05%).

2. Discussion

Results indicated that gold as the electrode substrate gives an ideal fuel efficiency, although the potential of the electrode was relatively low. This low electrode potential, however, may be attributed to the small surface area of the Pd catalyst that was electroplated and appeared grey rather than powdery black.

During the third quarter, the study will be expanded to inexpensive materials such as stainless steel and iron which have low activities as the hydrogen electrode.

C. TASK II. STUDY OF ELECTROLYTE

1. Background

This task was started at the beginning of the contract. The most effective factor on the anode activities, as indicated by the electrode potentials, was the activity of hydroxyl ions, OH^-, in the electrolyte. The slope of the anode potential vs log (A_{OH^-}) was about 0.087 volt. The kind of cation itself (except for Cs) had no significant effect. The anode potentials in CsOH electrolyte were less active than those in the other hydroxide electrolytes (hydroxides of Li, Na and K) having the same activities of hydroxyl ions.

Comparing the activities of hydroxyl ions and the ionic conductivities of these electrolytes at the same concentration, potassium hydroxide, was the best among those tested.

During this quarter, further investigation was carried out on the effects of concentrations of the electrolyte and fuel, temperature, and impurities in the KOH electrolyte. Impurities tested included the most probable ions in the system, $CO_3^=$, Cl^- and Fe^{++}.

2. Experimental Method

The experimental method was the same as that described in our previous report. The galvanostatic polarization curves were determined using the Kordesch-Marko bridge with solid nickel electrodes plated with 10 mg/in^2 of Pd black. The half cell used for the test is illustrated in Figure 2. The open circuit potential was taken when a steady potential was reached and the potential at each current was measured after exactly one minute of electrolysis at each value of the current, which was increased stepwise.

All electrolytes were made up by using reagent grade chemicals. Since these alkaline solutions contained a significant amount of H_2O, all solutions were analyzed by titration for OH^- ion concentration, and the proper amount of chemicals were added to obtain the exact strengths of the electrolyte desired.

For testing the effect of $CO_3^=$, a fresh bottle of granular KOH was used to prepare the carbonate-free 5M KOH solution. $CO_3^=$ ion was added to the solution by bubbling CO_2 gas through the solution. Free KOH and the total carbonate ions were then determined by a conventional titration with dilute HCl. Immediately after the analysis, a known amount of $N_2H_4 \cdot H_2O$ was added to the remaining solution to form a 2M N_2H_4 solution, and the polarization curve on the standard electrode (solid nickel with Pd black) was determined.

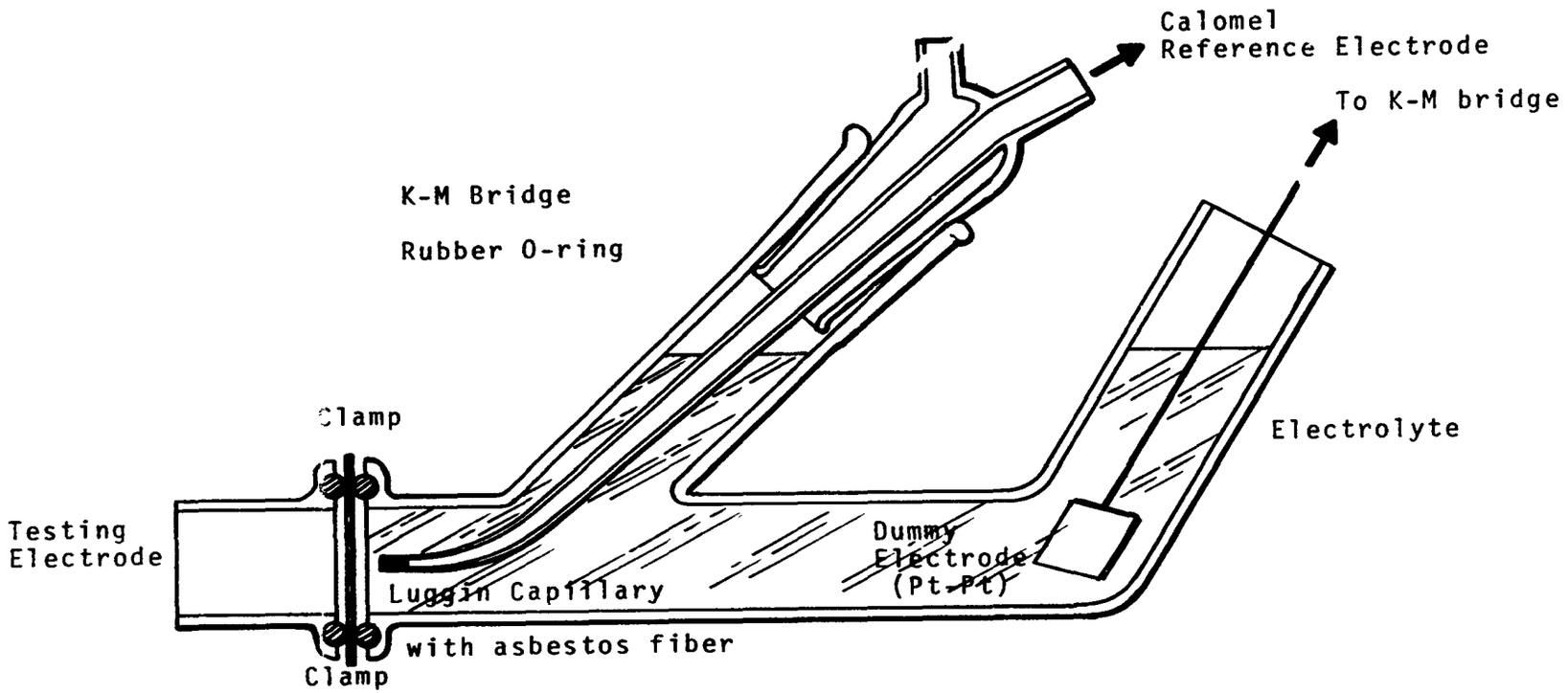

Figure 2. Half Cell for Polarization Study

Cl^- was added as KCl and Fe^{++} was added as $FeSO_4 \cdot 7\ H_2O$. Some colloidal precipitation of $Fe(OH)_2$ were observed when larger amounts of Fe^{++} were added to the KOH electrolyte.

3. Effect of Concentration of KOH and N_2H_4.

Data obtained supplement those obtained during the first quarter. Figure 3 indicates the characteristics of the hydrazine anode potential as a function of KOH concentration at various temperatures. For reference to the practical operation of the N_2H_4 - air fuel cell system, the hydrazine anode potentials at 100 ma/cm^2 at various conditions are also listed in Table 2.

The hydrazine anode potential increased linearly with the logarithm of the KOH activity. The slope of the potential increase, $dE/d\log(A_{OH^-})$, were estimated to be about 0.075 volt at 40°C and 0.07 volt at 70°C, although these values can vary since the points were somewhat scattered.

An increase of hydrazine concentration also increased the anode potential, but the effect was less than that caused by an increase in KOH activity.

The potential increased significantly when the temperature was raised to 60°C, but very little when it was raised from 60°C to 70°C.

4. Effect of Impurity Ions in the Electrolyte

a. Effect of $CO_3^=$.

The most characteristic data are summarized in Table 3 which indicates the small but definite loss of potential by CO_2 dissolution into the electrolyte.

b. Effect of Cl^-.

The effect of Cl^- was determined in 7M KOH with 2M N_2H_4 electrolyte. The electrode potentials at open-circuit and at 100 ma/cm^2 are shown in Figure 4 as a function of the concentration of Cl^-. Figure 4 shows that Cl^- had little or no effect on the hydrazine electrode potential.

e. Effect of Fe^{++}.

7M KOH with 2M N_2H_4 solution was used to determine the effect of Fe^{++}, which was added as $FeSO_4 \cdot 7\ H_2O$. Some precipitation of colloidal ferrous hydroxide, $Fe(OH)_2$, was observed above 10 ppm of Fe^{++} addition. Figure 5 shows the electrode potentials at open circuit and at 100 ma/cm^2 as a function of the concentration of Fe^{++}.

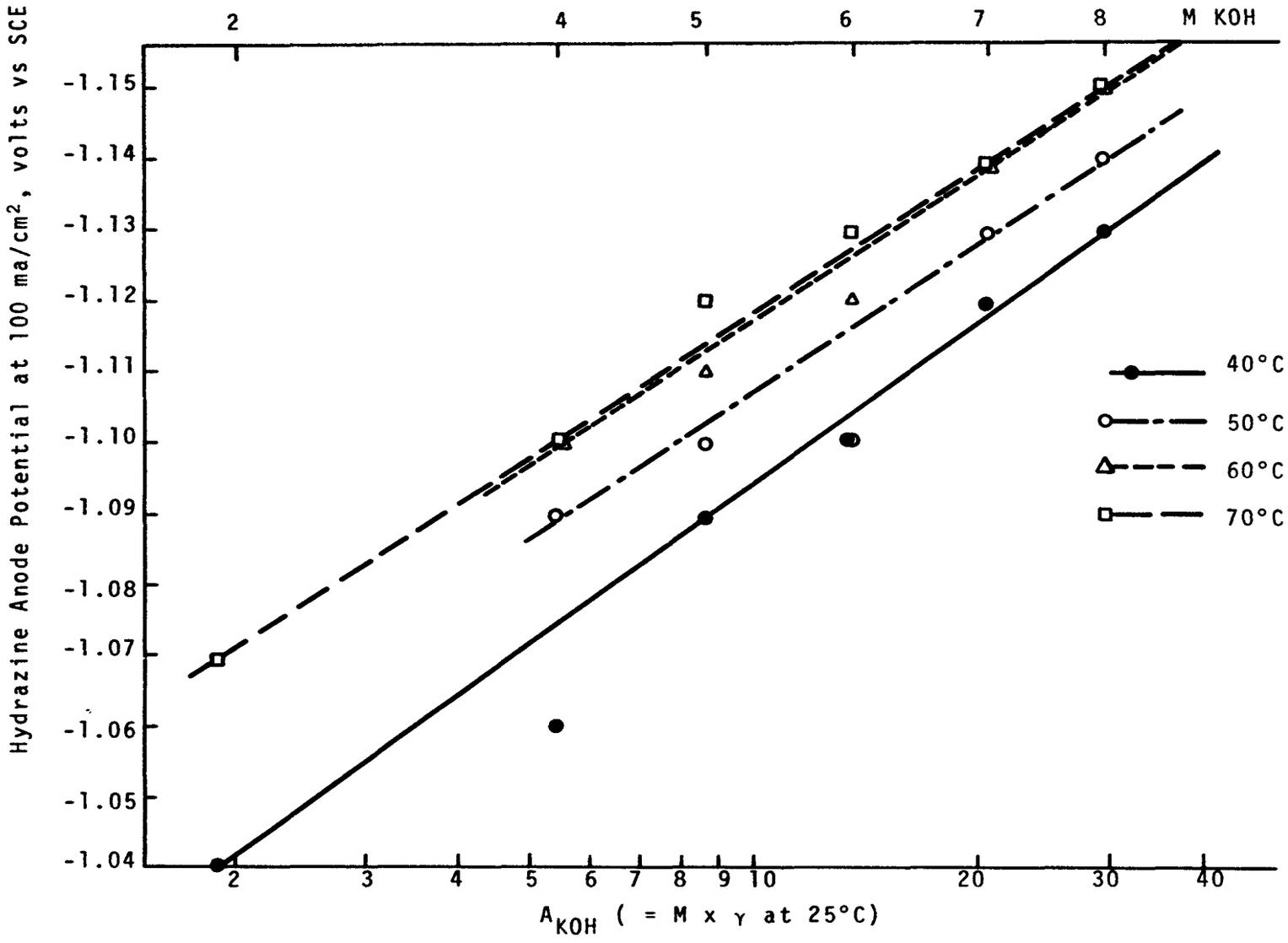

Figure 3. Effect of KOH Concentration on Hydrazine Anode Potential (N_2H_4:2M)

Table 2

EFFECT OF CONCENTRATION OF KOH AND N_2H_4 ON THE HYDRAZINE ANODE POTENTIAL AT 100 MA/CM^2, VOLTS VS SCE

KOH M	N_2H_4 M	Temperature 40°C	50°C	60°C	70°C
4.0	1.5	-1.05	-1.08	-1.09	-1.09
	2.0	-1.06	-1.09	-1.10	-1.10
	2.5	-1.04	-1.08	-1.10	-1.10
	3.0	-1.05	-1.08	-1.10	-1.12
5.0	1.5	-1.07	-1.10	-1.11	-1.12
	2.0	-1.09	-1.10	-1.11	-1.12
	2.5	-1.08	-1.10	-1.11	-1.13
	3.0	-1.06	-1.10	-1.13	-1.14
6.0	1.5	-1.06	-1.09	-1.10	-1.10
	2.0	-1.10	-1.10	-1.12	-1.13
	2.5	-1.11	-1.14	-1.15	-1.15
	3.0	-1.10	-1.13	-1.14	-1.14
7.0	1.5	-1.09	-1.11	-1.12	-1.12
	2.0	-1.12	-1.13	-1.14	-1.14
	2.5	-1.11	-1.14	-1.15	-1.15
	3.0	-1.13	-1.14	-1.15	-1.16
8.0	1.5	-1.13	-1.14	-1.15	-1.15
	2.0	-1.13	-1.14	-1.15	-1.15
	2.5	-1.12	-1.14	-1.15	-1.15
	3.0	-1.10	-1.13	-1.15	-1.15

Table 3

EFFECT OF $CO_3^=$ IN KOH ELECTROLYTE

Original Electrolyte: 5M KOH + 2M N_2H_4

CO_2 Addition	Molarity KOH	Molarity $CO_3^=$	Temp.°C.	OCP,V*	**Current Density, ma/cm² 50	100
No CO_2	4.64	---	50	-1.17	-1.10	-1.10
			70	-1.17	-1.12	-1.12
1 min bubbling at 0.5 l/min.	4.51	0.19	50	-1.14	-1.09	-1.09
			70	-1.14	-1.10	-1.10
5 min bubbling at 0.5 l/min.	2.76	0.95	50	-1.13	-1.06	-1.06
			70	-1.14	-1.07	-1.08
10 min bubbling at 0.5 l/min.	1.15	1.71	50	-1.14	-1.05	-1.05
			70	-1.14	-1.07	-1.07

*Open Circuit Potential vs Saturated Calomel Electrode
**Anode potential vs SCE.

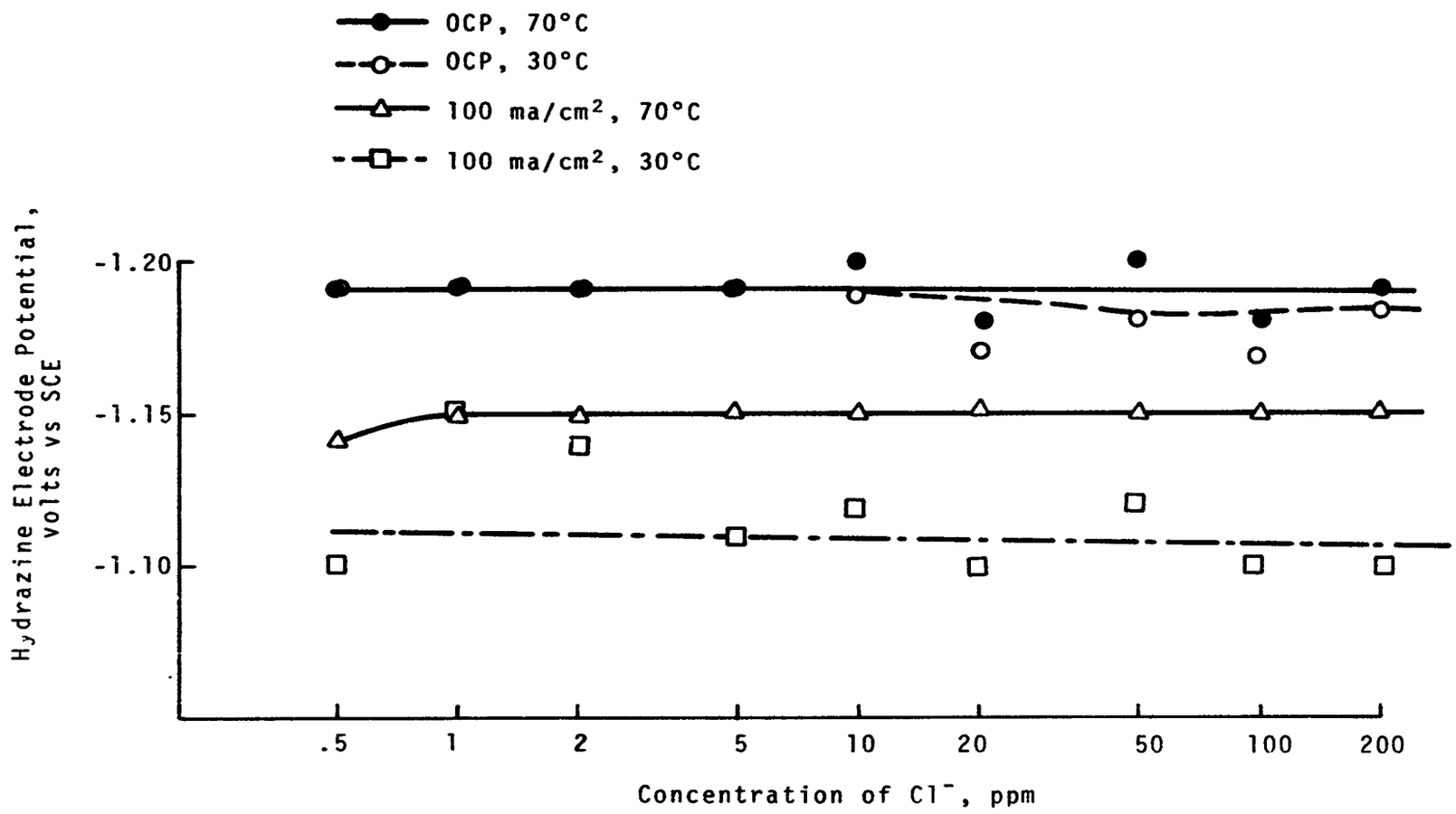

Figure 4. Effect of Cl^- on the Hydrazine Electrode Potential (7M KOH + 2M N_2H_4)

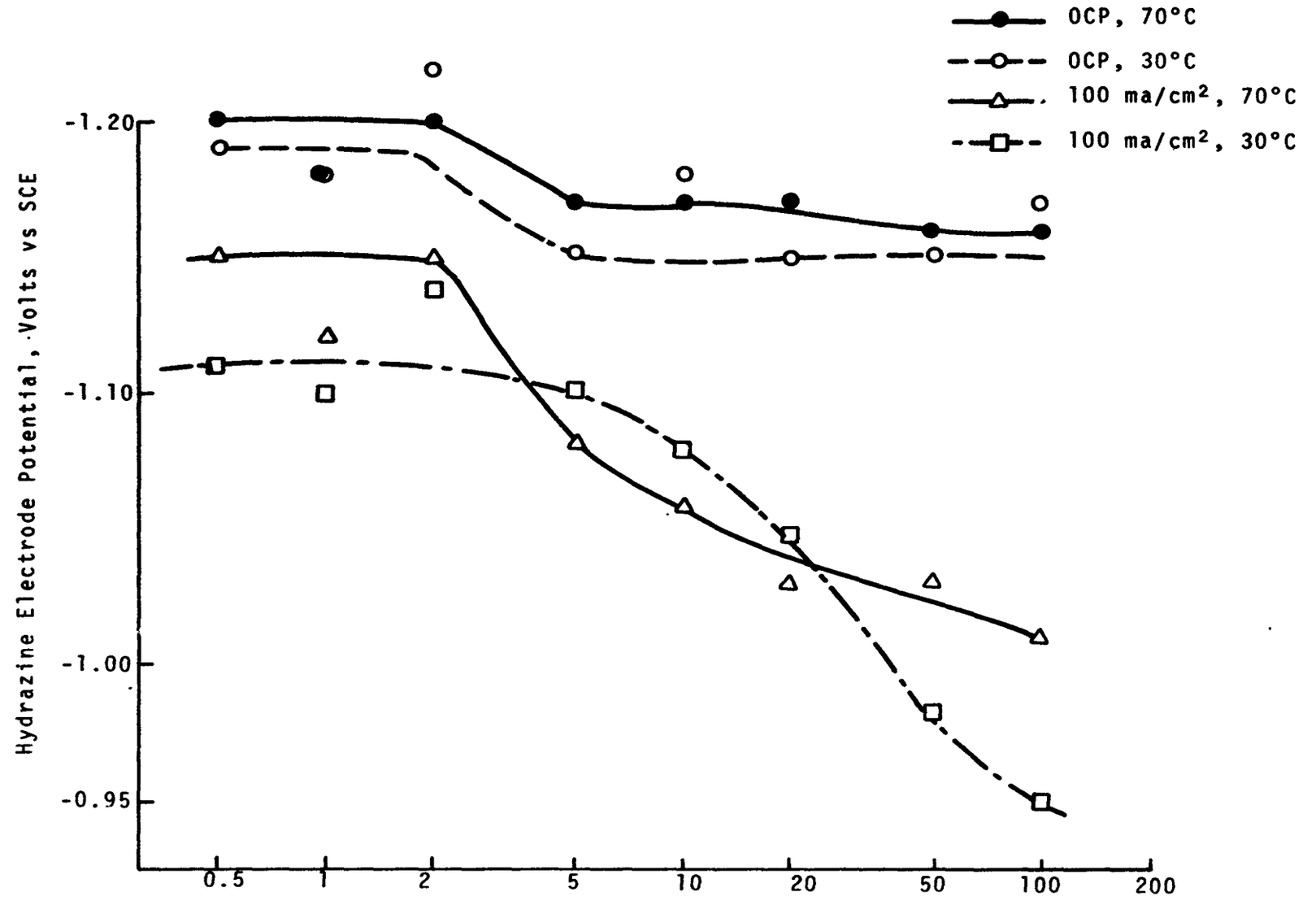

Figure 5. Effect of Fe^{++} on the Hydrazine Electrode Potential (7M KOH + 2M N_2H_4)

There was little or no effect of Fe^{++} up to 2 ppm, but the electrode potential at the operating condition dropped steeply with an increase in Fe^{++} concentration above 5 ppm. Although it is not certain, the precipitation of colloidal ferrous hydroxide might have accounted for this effect.

5. Conclusions

From the results obtained during this quarter, the following conclusions can be drawn:

(i) The hydrazine electrode potential linearly increases, becoming more anodic, with the logarithm of the hydroxyl electrolyte activity. The slope $dE/d\log(A_{OH^-})$ is 0.07 volt or larger for the temperature range tested.

(ii) The hydrazine electrode potential increases with increasing N_2H_4 concentration. The effect is less than that by the increase of hydroxyl in activity.

(iii) Dissolved CO_2 in the KOH electrolyte lowers the hydrazine electrode potential.

(iv) Cl^- in the electrolyte has little or no effect on the hydrazine electrode potential.

(v) Fe^{++} in the electrolyte has little or no effect on the hydrazine electrode potential up to 2 ppm of Fe^{++}, but the potential at the operating condition significantly dropped with increasing Fe^{++} concentration above 5 ppm.

D. TASK III. STUDY OF CATALYST POISONS

1. Experimental Method

During the second quarter two related groups of experiments were carried out to determine the feasibility of using catalyst poisons to improve the hydrazine electrode.

The first group of tests was the determination of polarization characteristics of the hydrazine electrode in the presence of the catalyst poisons, $S^=$, $Se^=$ and As^{5-}.

The second group of tests was the determination of the effect of catalyst poisons on the rate and composition of the gas evolved on the hydrazine electrode.

The first group was carried out in the half cell illustrated in Figure 2 by using solid nickel electrodes plated by electrolysis with 10 mg/in^2 of Pd black. The second group was carried out in the apparatus shown in Figure 6 by using porous nickel plaque

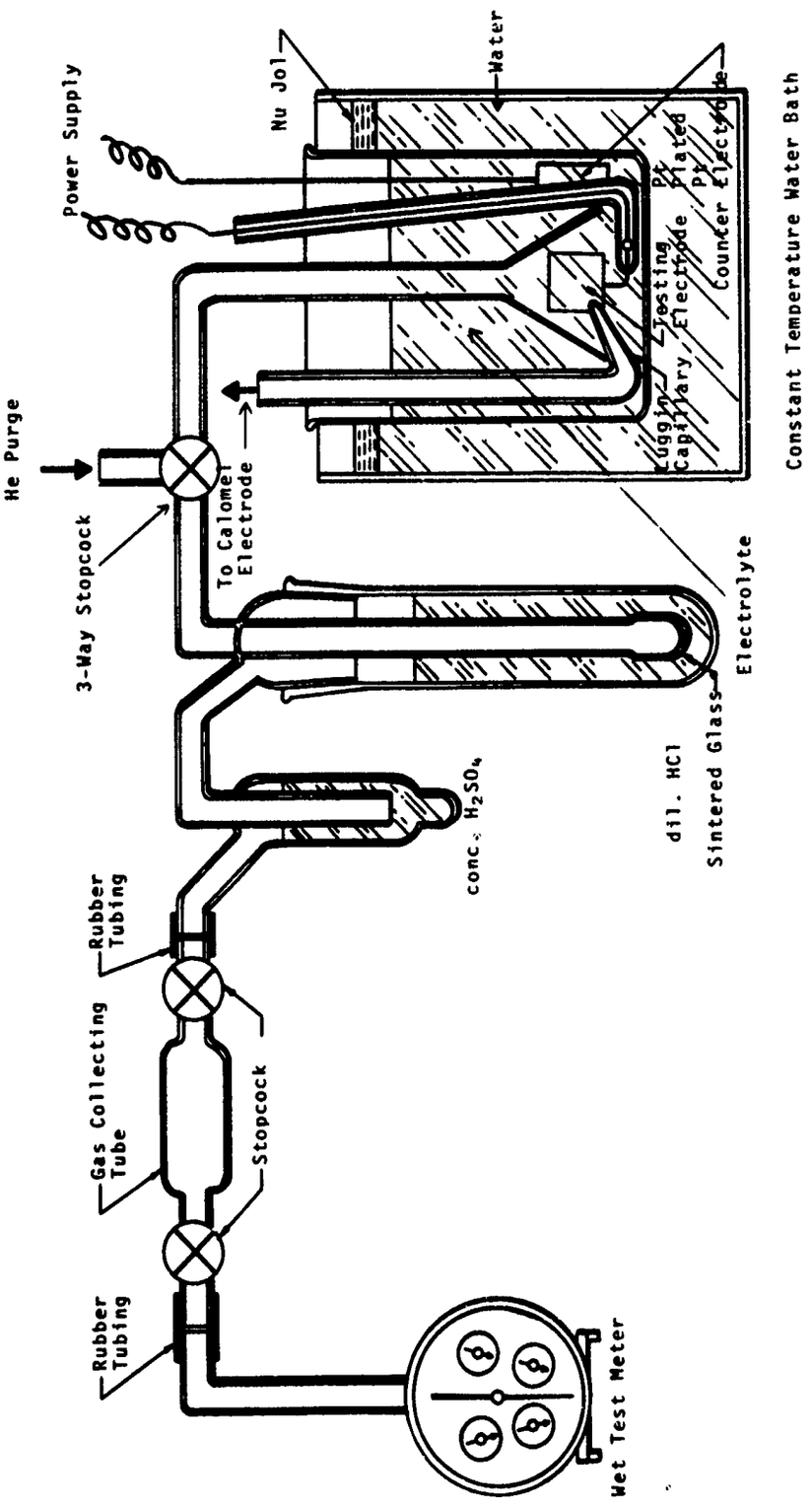

Figure 6. Reaction Generator and Gas Collecting Train

chemiplated with 10 mg/in^2 of Pd black. The electrolyte tested was 7M KOH + 2M N_2H_4 for the first group and 5M KOH + 2M N_2H_4 for the second group. $S^=$ and As^{5-} were added to the electrolyte from the stock solutions of Na_2S and As_2O_5. Since Na_2Se tends to precipitate by hydration, Na_2Se solution was freshly made for each test and added quickly to the electrolyte.

2. Results on Solid Nickel Electrode

Potentials at open circuit and at 100 ma/cm^2 are shown in Figures 7, 8, and 9 as a function of the concentrations of the catalyst poisons.

Results indicated a small but definite improvement in the potentials at very low concentrations of the poisons. However, the electrode lost activity sharply as the concentrations were further increased. The effect was most significant with $S^=$ followed by $Se^=$ and As^{5-}.

3. Results on Porous Nickel Electrode

The effects of the catalyst poisons on the rates of gas evolution at open circuit condition are given in Figure 10 as a function of the concentration of the poisons. Results indicated that the strongest effect was given by $S^=$ to decrease the rate of gas evolution, followed by $Se^=$, but no effect by As^{5-}. For $S^=$ and $Se^=$, a linear relation was observed between the logarithms of the rate of gas evolution and the concentration of these ions, up to approximately 5 x 10^{-3} mole/liter. Above this concentration, the gas evolution decreased more rapidly with an increase in the concentration of the catalyst poisons.

Analytical results on the evolved gas at 100 ma/cm^2 polarization in the electrolyte containing 5 x 10^{-3}M of the catalyst poisons are given in Table 4.

Results indicated that the addition of 5 x 10^{-3}M $S^=$ and $Se^=$ increased the fuel efficiency to practically 100% and decreased the NH_3 content in the exhaust gas one-half, although the loss of the electrode potential at 100 ma/cm^2 was about 0.2 volt from that of the electrode without the poisons. The effect of As^{5-} was much less than that of $S^=$ and $Se^=$.

The potentiostatic sweep curves on the electrode with $S^=$ and $Se^=$ under these conditions showed no peaks for the absorbed hydrogen.

4. Discussion

Results in general proved the validity of the approach developed in planning these tests. These results may even suggest a tentative mechanism for the effect of the poisons, although the

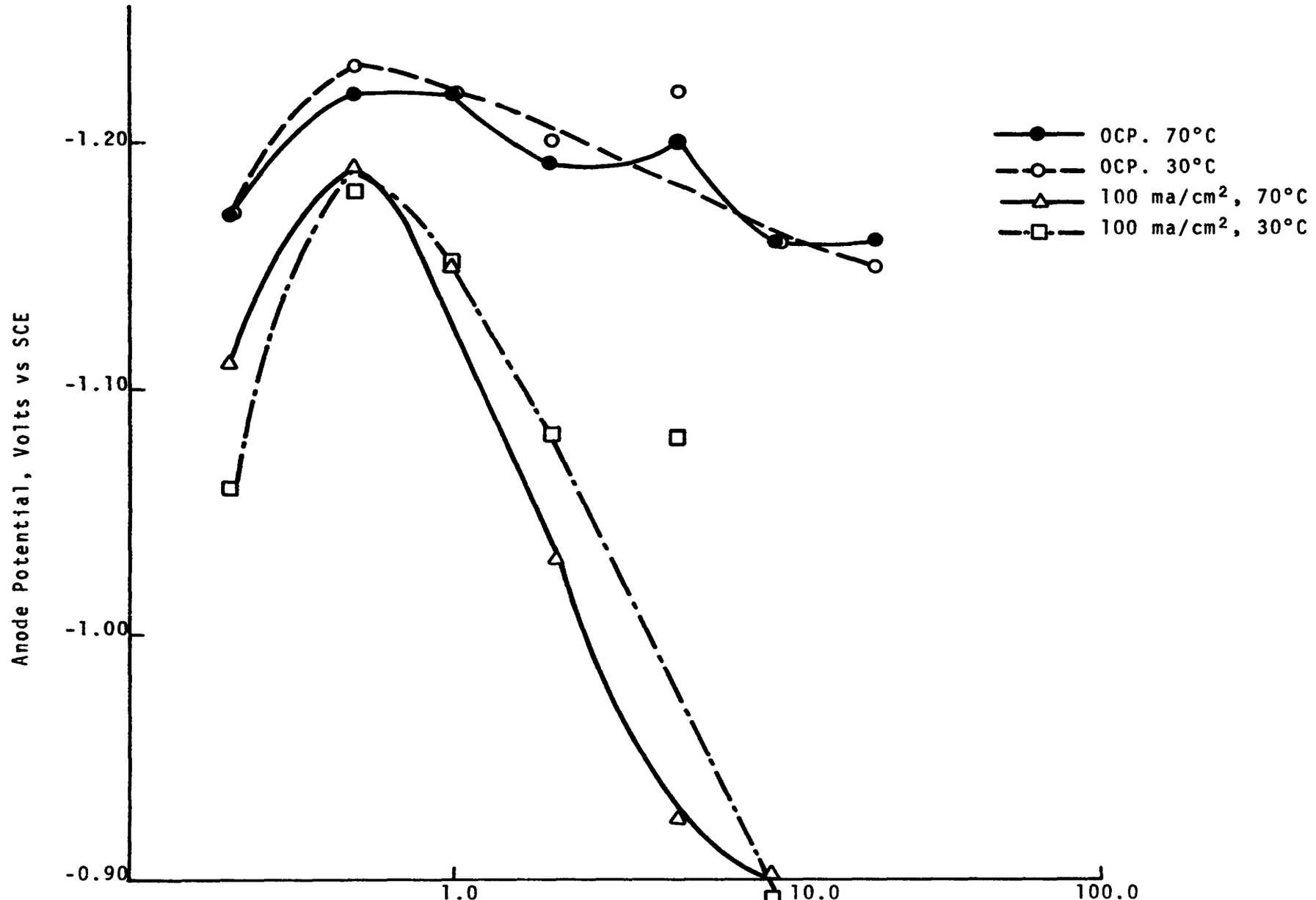

Figure 7. Effect of $S^{=}$ in the Electrolyte on the Polarization Characteristics of Hydrazine Electrode (7M KOH + 2M N_2H_4)

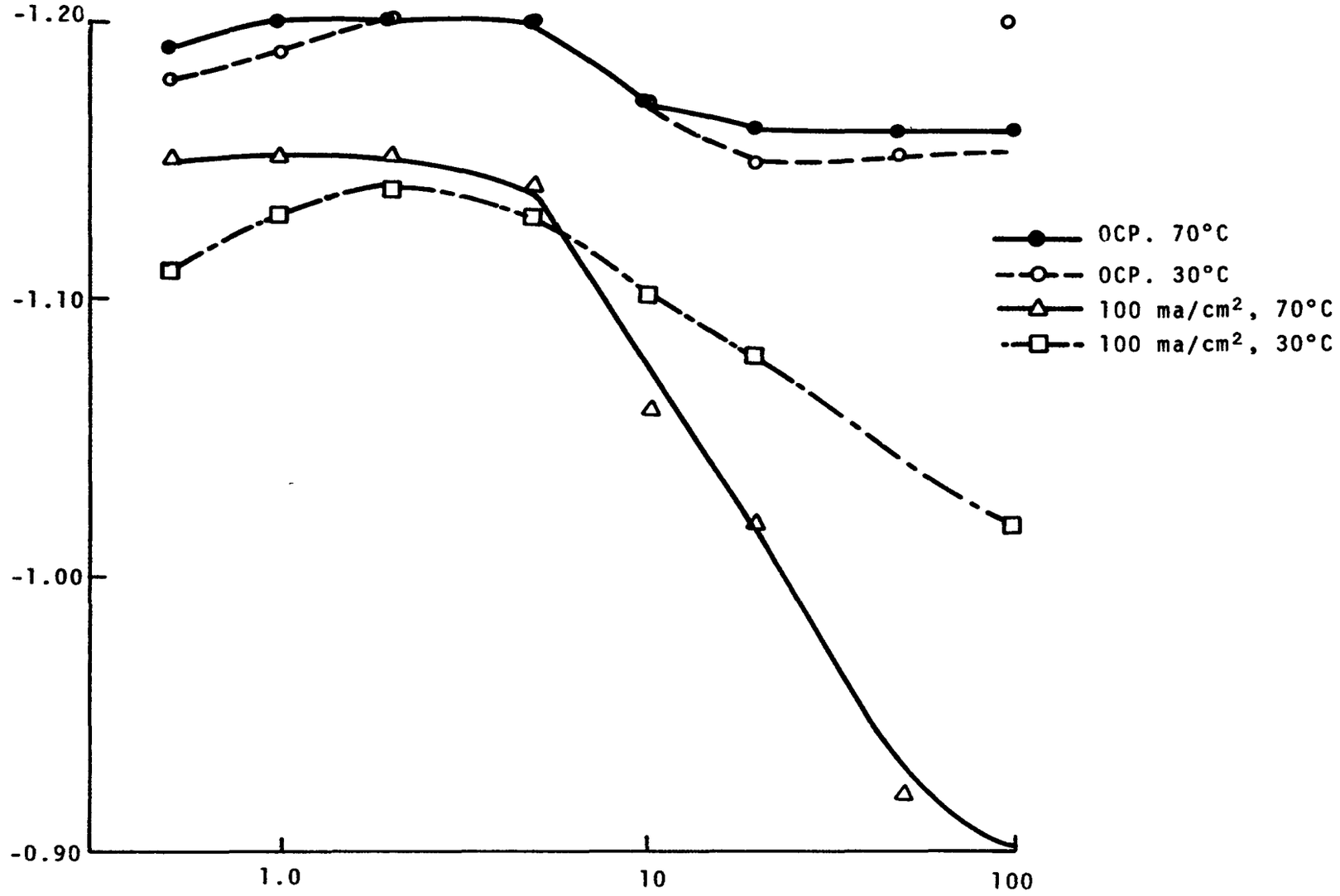

Figure 8. Effect of $Se^{=}$ in the Electrolyte on the Polarization Characteristics of Hydrazine Electrode (7M KOH + 2M N_2H_4)

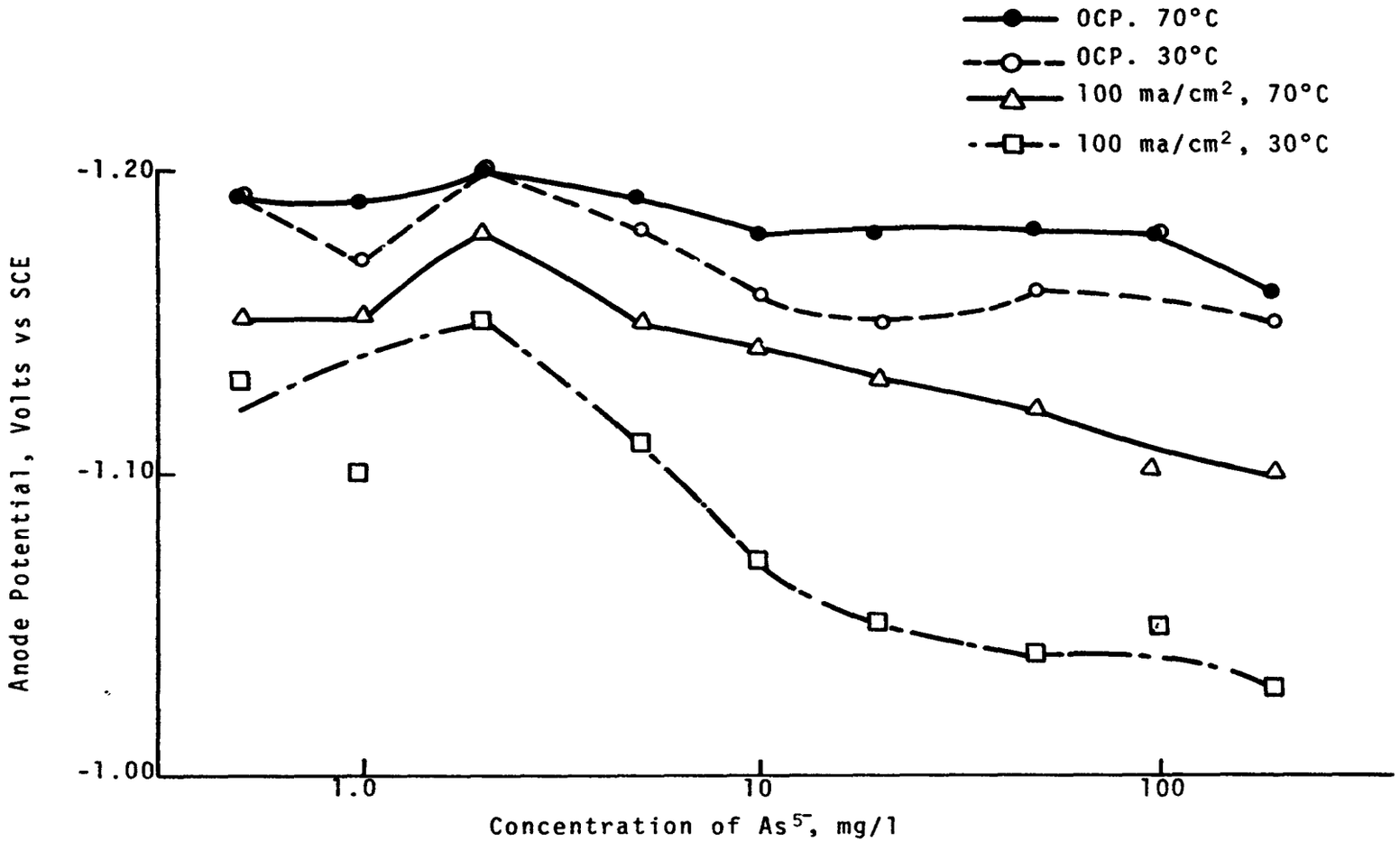

Figure 9. Effect of As^{5-} in the Electrolyte on the Polarization Characteristics of Hydrazine Electrode (7M KOH + 2M N_2H_4)

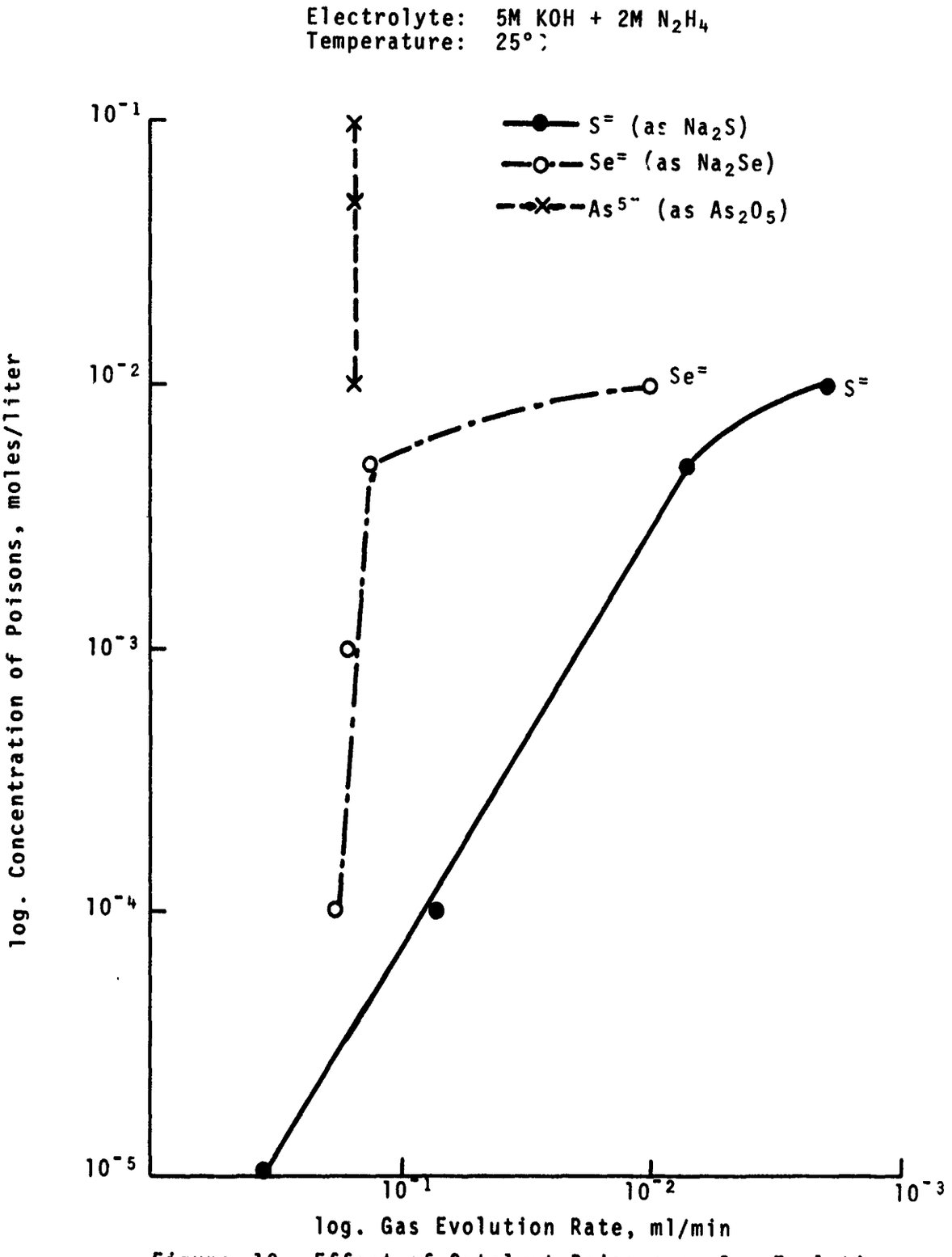

Figure 10. Effect of Catalyst Poisons on Gas Evolution Rate at Open Circuit Conditions

Table 4

THE EFFECT OF THE CATALYST POISONS ON THE COMPOSITION OF THE EVOLVED GAS AT 100 MA/CM^2 POLARIZATION

Electrolyte: 5M KOH + 2M N_2H_4 + Catalyst Poisons (1 x 10^3 M)

Catalyst Poison	Electrode Potential, at 100 ma/cm^2 Volts vs SCE	Gas Composition, % After NH_3 Extraction		NH_3 Content
		H_2	N_2	%
None	-1.24	27.8	72.2	0.39
$S^=$	-1.28 (OCP)	59.6	40.4	1.11
$S^=$	-1.05	1.1	98.9	0.22
$Se^=$	-1.04	Trace	99.5	0.21
As^{5-}	-1.20	12.0	88.0	0.52

study has not yet been concluded. The linear relation between the logarithms of the concentration of the catalyst poisons and the rate of the gas evolution is similar to the relation between the concentration of anodic type inhibitors necessary to passivate iron in an environment containing Cl^- or $SO_4^=$ (Ref. 2). The most likely mechanism for the phenomenon is then the competitive adsorption of two (ionic) species on the metal surface, in the present case the ions of the catalyst poison and atomic (or molecular) hydrogen liberated by the catalytic decomposition of N_2H_4. The plateau observed on the curve may be explained by this mechanism as the saturation of the adsorbed poison ions on the active hydrogen electrode sites. Under such conditions it is also obvious that no peak of the adsorbed hydrogen should be observed on the potentiostatic sweep curve on the electrode.

Results in Figures 7 to 10 and in Table 4 suggest that the optimization of the condition must consider the inverse effect of the loss of potential by the excess amount of the catalyst poisons.

During the third quarter the effort will be focussed on optimizing the concentration of the catalyst poisons and on the method of adding them to the electrode system.

E. TASK IV. STUDY OF INEXPENSIVE CATALYST

Experiments that were originally planned for this quarter included tests on metal chelate catalysts for the N_2H_4 anode. However, no electrode tests were carried out because of some difficulties encountered in preparing the electrodes incorporating these catalysts. The proprietary process used to prepare these electrodes involves various steps that must be closely controlled, and difficulties experienced were mainly concerned with these controls. At the end of the quarter, these difficulties had been solved and the experiments planned are all expected to be carried out during the third quarter.

F. TASK V. STUDY OF DECOMPOSITION OF NH_3

1. Background

The odor of ammonia (NH_3) is often very strong during the operation of N_2H_4 - air fuel cells. It is also known that an appreciable amount of NH_3 was formed by the thermal decomposition of N_2H_4, particularly over some specific catalysts such as cobalt metal (Refs. 3 and 4).

The quantitative determination of NH_3 in the gaseous reaction products on the hydrazine anode was carried out during the first quarter of the present program. Results of the analysis indicated that the amount of NH_3 averaged approximately 0.5% (volume) of the total gaseous products, independent of the current densities, up to 200 ma/cm^2, on the solid electrodes of various metals catalyzed

with Pd black. This result suggests that NH_3 was formed by an electrochemical reaction, either as one step in the oxidation of N_2H_4 to H_2O and N_2 or as an independent side reaction of the oxidation of N_2H_4.

The importance of NH_3 formation in the practical operation of the N_2H_4 - air fuel cells is principally in two areas:

(i) It causes a loss of fuel efficiency because of the incomplete oxidation of N_2H_4.

(ii) There is air polution by NH_3 escaping into the atmosphere.

Although the study of the electrode substrate suggested that some decrease in NH_3 formation might be obtained by selecting a proper substrate and catalyst, complete elimination of NH_3 from the anode reaction seems rather difficult. The present task was then added to study possible decomposition of NH_3 by means of oxidation with air over a catalyst.

2. Experimental Method

Figure 11 is a schematic diagram of the test apparatus.

Flow rates of N_2, NH_3, and air were individually adjusted by a needle valve and a flow meter on each supply line so that any mixture could be obtained. All tubing, fittings and valves, and the reactor, were made of 304 stainless steel. The reactor was a one-inch pipe approximately 15 inches long. It was heated uniformly from the outside by a heating tape. The temperature of the reaction zone, where catalyst powder was packed for about 3" long at the center of the tube, was adjusted within $\pm$ 3°C of a desired temperature. The analysis of NH_3 was made before and after the reactor tubing. For the analysis, the gas was introduced for a certain period into a known amount of 0.1N HCl and the unreacted HCl was back-titrated with a known concentration (0.1N) of NaOH solution.

3. Results

First, some commercial catalysts were tested in the condition that simulates the relatively high concentration of NH_3 in medium size fuel cell systems of few hundreds watts. The flow rates of the testing gas were 1 liter/min. of N_2 mixed with about 15 cc/min of NH_3. The flow rate of air mixed with the above gas stream was 185 cc/min. This amount contains approximaately four times the oxygen necessary to complete the following desirable reaction:

$$2\ NH_3 + 3/2\ O_2 \rightarrow 3\ H_2O + N_2 \qquad (1)$$

Table 5 gives the results. Data are for an average of at least two runs.

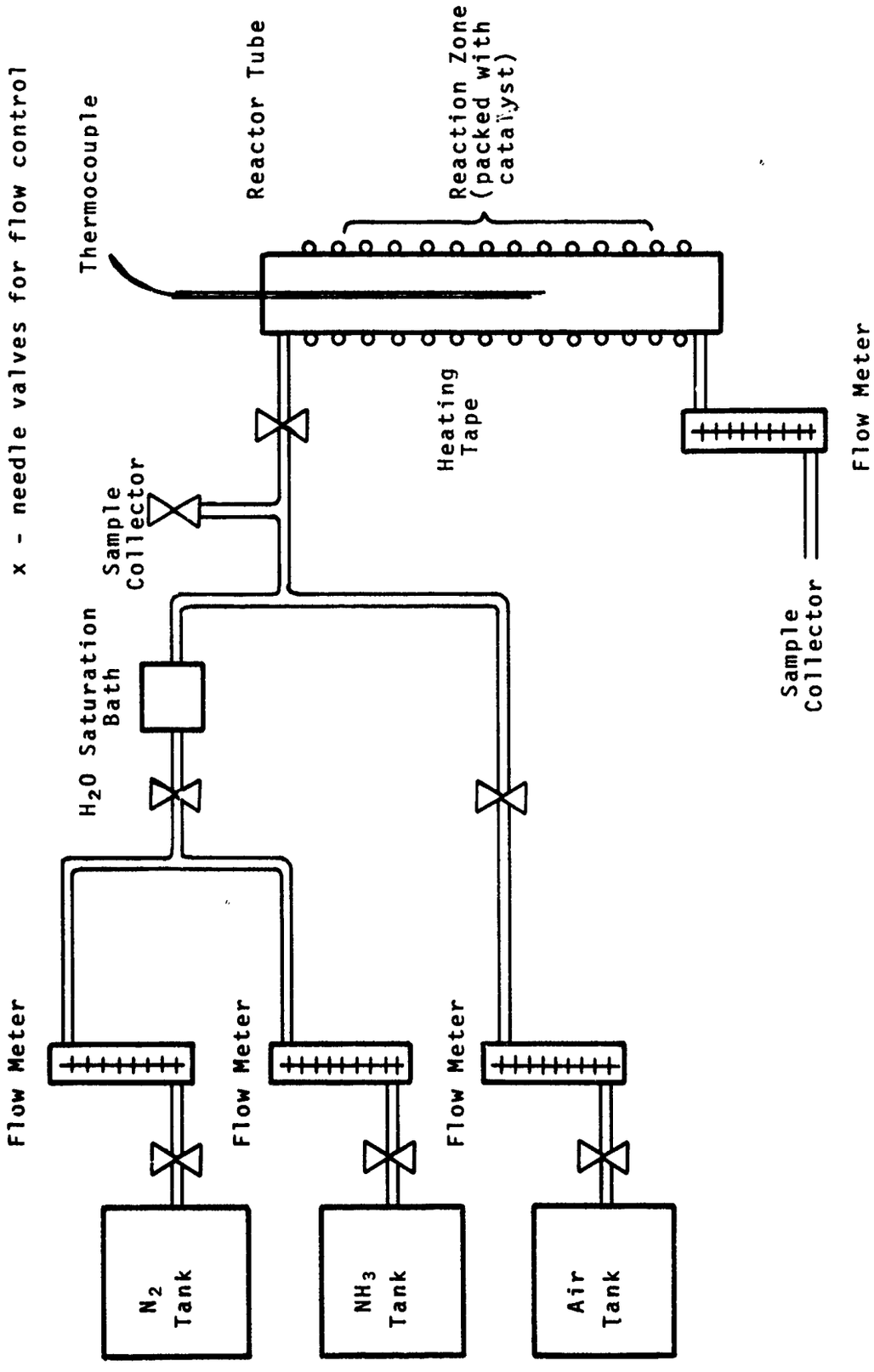

Figure 11. Schematic Diagram of an Apparatus for NH_3 Decomposition Test

Table 5

NH_3 DECOMPOSITION "1"

Gas Composition: N_2 = 1,000 cc/min.
NH_3 = 15 cc/min.
Air = 185 cc/min.

Catalyst	Temp., °C	% Conversion of NH_3
Al_2O_3 (Control)	30	None
Al_2O_3	100	None
1.0% Rh on Al_2O_3	30	2.6
1.0% Rh on Al_2O_3	100	None
Girdler Catalyst G-49*B	100	None
Girdler Catalyst G-66**P	100	None
Girdler Catalyst G-42***	100	None

*Reduced - Stabilized Li-Ni Catalyst
**Low Temperature Shift Conversion Catalyst
***Promoted Iron Oxide Catalyst
Girdler: Girdler Catalysts, Louisville, Ky.

Since the results showed very low or no conversion under those conditions, the NH_3 content was then increased almost six times by cutting N_2 stream in order to determine more clearly the difference.

Results so far indicate that Pt was the only usable catalyst in this system and the highly loaded Pt catalyst (Ni-Pt in Table 6 and 7) could decompose almost 99% of NH_3 in the gas stream containing originally about 7.5% of NH_3.

This work will be further continued in the third quarter.

Table 6

NH_3 DECOMPOSITION "2"

Gas Composition: NH_3 = 15 cc/min.
Air = 185 cc/min.

Catalyst	Temp.,°C	% Conversion of NH_3
Girdler G-42 catalyst*	100	None
Girdler G-43 catalyst**	100	21.0
Pt - Ni***	100	83.0

*Promoted Iron Oxide Catalyst
**Promoted Pt Catalyst
***0.030 in. thick Ni plaque was chemi-plated with 100 ma/in^2 of Pt. and then crushed into small pieces.

Table 7

NH_3 DECOMPOSITION "3"

Gas Composition: NH_3 - 15 cc/min. presaturated with H_2O vapor at 70°C
Air - 185 cc/min.

Catalyst	Temp., °C	% Conversion of NH_3
Pt - Ni*	100	98.6
Pt - Ni*	50	None
Harshaw Cobalt Catalyst	100	26.8
Harshaw Zinc Catalyst	100	None
Harshaw Vanadium Catalyst	100	None
Harshaw Cr-Al_2O_3 Catalyst	100	None
Raney Ni-Pt**	100	None
Raney Ni-Pt***	100	None

*Same as one in Table 6
**Raney Ni with absorbed H_2 was chemi-plated with Pt (1% wt.).
***Raney Ni without absorbed H_2 was chemi-plated with Pt (1% wt.).

Harshaw: Harshaw Catalyst, Cleveland, Ohio.

III. PHASE II - INVESTIGATION OF SEPARATOR

A. EXPERIMENTAL METHOD

The apparatus and the experimental method were the same as those used in the first quarter. Figure 3 shows the half cell testing unit. Separators tested were placed on the front of the electrolyte surface side of our MRC cathode (proprietary) and a sheet of nylon cloth was added to the front of the asbestos separator to prevent excess swelling of the asbestos.

The electrolyte was 5M KOH solution containing 2M N_2H_4. The air cathode polarization curves were taken at 30, 50, and 70°C by using an interrupting bridge (Kordesch-Marko bridge) in order to determine IR free potential and IR drop through the asbestos separator (between Luggin Capillary and the cathode). During the testing the air flow rate was kept constant at 60 cc/min.

B. ASBESTOS SEPARATOR

Two types of commercial asbestos, each of two thicknesses (10 and 15 mils) were tested. Other tests included those on multiple layers of these separators; two and three layers of asbestos papers were compressed together under 24,000 psi pressure and were used like a single sheet of separator.

One 15 mil chrysotile paper was impregnated with MgO and tested for improvement. For this treatment, the paper was first soaked with $MgCl_2$ solution. Then it was dried in an oven, treated with NH_4OH solution, dried, and finally heated at 400°C in an oven.

Results are summarized in Table 8.

C. NON-ASBESTOS SEPARATOR

Two non-asbestos separators were tested. One was thoria powder bonded with Teflon. The other was a thin alkaline battery separator made of polymer.

Results are summarized in Table 8, together with those on the asbestos separators.

D. DISCUSSION

The open circuit potentials and IR-free potentials can be used to estimate the protective abilities of the separators against N_2H_4 poisoning and IR drop can be used to estimate the ionic conductivity through the separators.

If we could assume that the essential electrode activities, without influences of the N_2H_4 poisoning and of the diffusion characteristics

Table 8

SUMMARY OF SEPARATOR TESTS

Electrolyte: 5M KOH + 2M N_2H_4
Temp: 30°C

Separator	O.C.P., Volts	IR Free Potential, volt, at various C.D., ma/cm²			IR Drop, volt, at 100 ma/cm²
		50	100	200	
Fuel Cell Grade*, 15 mil (control)	-0.245	-0.255	-0.275	-0.345	0.185
Fuel Cell Grade, 10 mil, 1 layer	-0.245	-0.260	-0.270	-0.315	0.180
Fuel Cell Grade, 10 mil, 2 layer	-0.250	-0.260	-0.275	-0.315	0.200
Fuel Cell Grade, 10 mil, 3 layer	-0.255	-0.270	-0.275	-0.315	0.890
Acco #1**, 15 mil, 1 layer	-0.230	-0.240	-0.250	-0.280	0.225
Acco #1, 15 mil, 2 layer	-0.225	-0.250	-0.260	-0.300	0.220
Acco #1, 15 mil, 3 layer	-0.225	-0.240	-0.260	-0.300	0.230
Acco #1, 10 mil, 1 layer	-0.240	-0.245	-0.265	-0.360	0.240
Acco #1, 10 mil, 2 layer	-0.235	-0.260	-0.295	-0.495	0.295
Acco #1, 10 mil, 3 layer	-0.245	-0.270	-0.285	-0.335	0.240
Fuel Cell Grade, 15 mil, with MgO	-0.240	-0.250	-0.260	-0.300	0.255
Thoria Matrix†	-0.240	-0.270	-0.280	-0.340	0.230
Alkali Battery Separator††	-0.245	-0.285	-0.290	-0.380	0.190
Temp: 50°C					
Fuel Cell Grade*, 15 mil, (control)	-0.215	-0.235	-0.250	-0.315	0.165
Fuel Cell Grade, 10 mil, 1 layer	-0.220	-0.240	-0.250	-0.305	0.170
Fuel Cell Grade, 10 mil, 2 layer	-0.215	-0.235	-0.250	-0.290	0.165
Fuel Cell Grade, 10 mil, 3 layer	-0.220	-0.240	-0.250	-0.285	0.530
Acco #1**, 15 mil, 1 layer	-0.225	-0.240	-0.240	-0.285	0.200
Acco #1, 15 mil, 2 layer	-0.205	-0.235	-0.245	-0.300	0.265
Acco #1, 15 mil, 3 layer	-0.200	-0.230	-0.245	-0.300	0.275
Acco #1, 10 mil, 1 layer	-0.240	-0.245	-0.260	-0.360	0.155
Acco #1, 10 mil, 2 layer	-0.220	-0.255	-0.280	-0.320	0.185
Acco #1, 10 mil, 3 layer	-0.210	-0.245	-0.260	-0.320	0.295
Fuel Cell Grade, 15 mil, with MgO	-0.205	-0.230	-0.240	-0.275	0.200
Thoria Matrix†	-0.220	-0.240	-0.250	-0.320	0.170
Alkali Battery Separator††	-0.235	-0.255	-0.270	-0.640	0.135
Temp: 70°C					
Fuel Cell Grade*, 15 mil, (control)	-0.210	-0.225	-0.240	-0.300	0.150
Fuel Cell Grade, 10 mil, 1 layer	-0.210	-0.235	-0.250	-0.300	0.175
Fuel Cell Grade, 10 mil, 2 layer	-0.215	-0.235	-0.240	-0.280	0.140
Fuel Cell Grade, 10 mil, 3 layer	-0.215	-0.235	-0.250	-0.280	0.430
Acco #1**, 15 mil, 1 layer	-0.225	-0.245	-0.250	-0.315	0.225
Acco #1, 15 mil, 2 layer	-0.185	-0.235	-0.260	-0.340	0.395
Acco #1, 15 mil, 3 layer	-0.195	-0.225	-0.240	-0.310	0.310
Acco #1, 10 mil, 1 layer	-0 95	-1.01	-1.02	-1.02	0.160
Acco #1, 10 mil, 2 layer	-0.87	-1.00	-1.00	-1.01	0.120
Acco #1, 10 mil, 3 layer	-0.190	-0.245	-0.265	-0.325	0.495
Fuel Cell Grade, 15 mil, with MgO	-0.200	-0.220	-0.235	-0.265	0.170
Thoria Matrix†	-0.195	-0.240	-0.270	-0.375	0.265
Alkali Battery Separator††	-0.215	-0.245	-0.275	-0.560	0.170

All volt data are vs. Saturated Calomel Electrode at 25°C
OCP: Open Circuit Potential vs. Saturated Calomel Electrode

* Supplied from Johns Mansville Co.
** Supplied from American Cyanamid Co.
† Supplied from Chemcell Co.
†† Supplied from Radiation Applications, Inc. (Permion Separator)

of the electrolyte through the separator, are same on these electrodes, the more negative potentials are the result mainly of N_2H_4 poisoning and partly of a change of the electrolyte condition on the surface by adding a separator on the front of the electrode surface.

In general, we might conclude from these data that the effect of N_2H_4 poisoning and the increase of IR drop are opposite. For example, the fuel cell grade asbestos separator treated with MgO showed the less influence of N_2H_4 poisoning, but at the same time an increase of IR drop, comparing with one without MgO. Consequently, the proper selection of the separator for the present system must consider both factors as well as the useful life of the material in the electrolyte which has not yet been tested.

From the data in Table 8, the fuel cell grade asbestos separator (1 layer of either 10 or 15 mils) seems somewhat better than other materials tested, although the separators, particularly thoria matrix and permion separator, indicated very competitive characteristics.

The work of this phase will be still continued in the third quarter.

IV. WORK PLANNED FOR THE THIRD QUARTER

Work planned for the third quarter includes the following:

(i) Continue the study of the electrode substrate materials including stainless steel and iron.

(ii) Continue the study of the catalysts.

(iii) Continue the study of the catalyst poisons, particularly the optimization of the use of the catalyst poisons.

(iv) Continue the study of NH_3 decomposition.

(v) Continue the study of the separator material.

(vi) Study the effects of impurity ions and the catalyst poisons on the air cathode performance.

We are expecting to reach certain conclusions on these studies at the end of the third quarter.

V. REFERENCES

1. S. Matsuda, Unpublished data obtained at Corrosion Lab., M.I.T., under supervision of Prof. H. H. Uhlig.

2. S. Matsuda and H. H. Uhlig, J. Electrochem. Soc., 111 Feb,(1964).

3. N. P. Keier, et al., Kinetika i Kataliz, 2:4, 509-518 (1961).

4. R. F. Drake, et al., "Study of Fuel Cells Using Storable Rocket Propellants", NASA Report CR-54428, under the contract NAS3-6476, Feb. 18 - May 17 (1965).

VI. IDENTIFICATION OF PERSONNEL

Name	Title	Hours
J. O. Smith	Manager	20
S. Matsuda	Project Leader	305
S. Brown	Res. Chemist	322
B. Sullivan	Res. Chemist	506
M. Lehman	Res. Chemist	32
T. Linxweiler	Tech. Editor	7
D. Manolagas	Draftsman	48
R. Regan	Technician	5
	Total	1245

Unclassified

Security Classification

DOCUMENT CONTROL DATA - R&D

(Security classification of title, body of abstract and indexing annotation must be entered when the overall report is classified)

1. ORIGINATING ACTIVITY (Corporate author) Monsanto Research Corporation, Boston Laboratory, Everett, Mass. 02149	2a. REPORT SECURITY CLASSIFICATION Unclassified 2b. GROUP none

3. REPORT TITLE

Investigation of Hydrazine-Air Fuel Cell Systems

4. DESCRIPTIVE NOTES (Type of report and inclusive dates)

Progress Report No. 2 15 May - 15 August 1966

5. AUTHOR(S) (Last name, first name, initial)

Matsuda, S.; Brown, S.P.; Smith, J. O.; and Sullivan, B. P.

6. REPORT DATE	7a. TOTAL NO. OF PAGES	7b. NO. OF REFS
February 1967	35	4

8a. CONTRACT OR GRANT NO. DA 28-043-AMC-01996(E) b. PROJECT NO. 1C6-22001-A-053-04 c. Task 12 d.	9a. ORIGINATOR'S REPORT NUMBER(S) MRB4035Q2 9b. OTHER REPORT NO(S) (Any other numbers that may be assigned this report) Technical Report ECOM-01996-2

10. AVAILABILITY/LIMITATION NOTICES

Each transmittal of this document outside the Dept. of Defense must have prior approval of the CG, U.S. Army Electronics Command, Fort Monmouth, New Jersey, Attn: AMSEL-KL-PC

11. SUPPLEMENTARY NOTES	12. SPONSORING MILITARY ACTIVITY U. S. Army Electronics Command Fort Monmouth, New Jersey 07703 AMSEL-KL-PC

13. ABSTRACT

Fuel efficiency of the hydrazine-air fuel cell system can be significantly increased by selecting a proper electrode substrate. It must be a poor hydrogen electrode material, according to the mixed potential concept. Both the anode potential and the fuel efficiency were improved by applying a minute amount of catalyst poisons such as $S^{=}$ and $Se^{=}$. The anode potential was increased by increasing the concentration of KOH and N_2H_4 in the electrolyte. The anode potential was no affected by Cl^{-} up to 200 mg/l, but it was lowered by $CO_3^{=}$ and Fe^{++} in the electrolyte. NH_3 in the exhaust gas from the anode was satisfactorily decomposed by Pt catalyst. In addition to fuel cell grade asbestos separator, which has given the best results, some non-asbestos separators such as ThO_2 membrane and alkaline battery separator also showed the promising results for the N_2H_4 - air system.

DD FORM 1 JAN 64 1473

Unclassified

Security Classification

14. KEY WORDS	LINK A		LINK B		LINK C	
	ROLE	WT	ROLE	WT	ROLE	WT
Fuel cells Hydrazine Electrocatalysts Electro-oxidation Fuel cell electrolytes Fuel cell reactions Hydrazine-air fuel cell						

INSTRUCTIONS

1. **ORIGINATING ACTIVITY:** Enter the name and address of the contractor, subcontractor, grantee, Department of Defense activity or other organization *(corporate author)* issuing the report.

2a. **REPORT SECURITY CLASSIFICATION:** Enter the overall security classification of the report. Indicate whether "Restricted Data" is included. Marking is to be in accordance with appropriate security regulations.

2b. **GROUP:** Automatic downgrading is specified in DoD Directive 5200.10 and Armed Forces Industrial Manual. Enter the group number. Also, when applicable, show that optional markings have been used for Group 3 and Group 4 as authorized.

3. **REPORT TITLE:** Enter the complete report title in all capital letters. Titles in all cases should be unclassified. If a meaningful title cannot be selected without classification, show title classification in all capitals in parenthesis immediately following the title.

4. **DESCRIPTIVE NOTES:** If appropriate, enter the type of report, e.g., interim, progress, summary, annual, or final. Give the inclusive dates when a specific reporting period is covered.

5. **AUTHOR(S):** Enter the name(s) of author(s) as shown on or in the report. Enter last name, first name, middle initial. If military, show rank and branch of service. The name of the principal author is an absolute minimum requirement.

6. **REPORT DATE:** Enter the date of the report as day, month, year; or month, year. If more than one date appears on the report, use date of publication.

7a. **TOTAL NUMBER OF PAGES:** The total page count should follow normal pagination procedures, i.e., enter the number of pages containing information.

7b. **NUMBER OF REFERENCES:** Enter the total number of references cited in the report.

8a. **CONTRACT OR GRANT NUMBER:** If appropriate, enter the applicable number of the contract or grant under which the report was written.

8b, 8c, & 8d. **PROJECT NUMBER:** Enter the appropriate military department identification, such as project number, subproject number, system numbers, task number, etc.

9a. **ORIGINATOR'S REPORT NUMBER(S):** Enter the official report number by which the document will be identified and controlled by the originating activity. This number must be unique to this report.

9b. **OTHER REPORT NUMBER(S):** If the report has been assigned any other report numbers *(either by the originator or by the sponsor)*, also enter this number(s).

10. **AVAILABILITY/LIMITATION NOTICES:** Enter any limitations on further dissemination of the report, other than those imposed by security classification, using standard statements such as:

(1) "Qualified requesters may obtain copies of this report from DDC."

(2) "Foreign announcement and dissemination of this report by DDC is not authorized."

(3) "U. S. Government agencies may obtain copies of this report directly from DDC. Other qualified DDC users shall request through _____."

(4) "U. S. military agencies may obtain copies of this report directly from DDC. Other qualified users shall request through _____."

(5) "All distribution of this report is controlled. Qualified DDC users shall request through _____."

If the report has been furnished to the Office of Technical Services, Department of Commerce, for sale to the public, indicate this fact and enter the price, if known.

11. **SUPPLEMENTARY NOTES:** Use for additional explanatory notes.

12. **SPONSORING MILITARY ACTIVITY:** Enter the name of the departmental project office or laboratory sponsoring *(paying for)* the research and development. Include address.

13. **ABSTRACT:** Enter an abstract giving a brief and factual summary of the document indicative of the report, even though it may also appear elsewhere in the body of the technical report. If additional space is required, a continuation sheet shall be attached.

It is highly desirable that the abstract of classified reports be unclassified. Each paragraph of the abstract shall end with an indication of the military security classification of the information in the paragraph, represented as *(TS)*, *(S)*, *(C)*, or *(U)*.

There is no limitation on the length of the abstract. However, the suggested length is from 150 to 225 words.

14. **KEY WORDS:** Key words are technically meaningful terms or short phrases that characterize a report and may be used as index entries for cataloging the report. Key words must be selected so that no security classification is required. Identifiers, such as equipment model designation, trade name, military project code name, geographic location, may be used as key words but will be followed by an indication of technical context. The assignment of links, roles, and weights is optional.